

Multipole effects of Γ_3 doublet– Γ_4 triplet states in PrMg₃Koji Araki,* Yuichi Nemoto, Mitsuhiro Akatsu, Shinya Jumonji, and Terutaka Goto
Graduate School of Science and Technology, Niigata University, Niigata 950-2181, Japan

Hiroyuki S. Suzuki

National Institute for Materials Science, Tsukuba 305-0047, Japan

Hiroshi Tanida

Graduate School of Advanced Sciences of Matter, Hiroshima University, Higashi-Hiroshima 739-8530, Japan

Shigeru Takagi

Physics Department, Graduate School of Science, Tohoku University, Sendai 980-8578, Japan

(Received 29 October 2010; revised manuscript received 22 April 2011; published 7 July 2011)

Elastic properties of cubic PrMg₃ with a non-Kramers Γ_3 doublet ground state have been investigated with ultrasonic measurements. The temperature dependence of the elastic constant $(C_{11}-C_{12})/2$ in PrMg₃ exhibits a characteristic minimum around 28 K and successively shows pronounced softening below 8 K down to 20 mK. The observation is well described by multipole susceptibility considering both an electric quadrupole O_v and electric hexadecapole H_v with Γ_{3g} representation for the crystal field level Γ_3 ground state and Γ_4 triplet excited state located at 54 K for PrMg₃. The contribution of the hexadecapole in the Γ_3 - Γ_4 system to the multipole susceptibility should be emphasized to explain a common feature of the minimum typically observed in $(C_{11}-C_{12})/2$ of Pr-based compounds PrPb₃, PrAg₂In, and the present PrMg₃, as revealed by systematic ultrasonic measurements.

DOI: [10.1103/PhysRevB.84.045110](https://doi.org/10.1103/PhysRevB.84.045110)

PACS number(s): 71.27.+a, 71.20.Eh, 62.20.de, 71.70.Ch

I. INTRODUCTION

Rare-earth compounds based on Pr ions with $4f^2$ orbitals have received much attention, because exotic phenomena associated with quadrupole ordering, heavy-fermion quasiparticles, unconventional superconductivity, and rattling of guest Pr ions in a cage have been recently reported.¹⁻⁴ A cubic crystal electric field (CEF) splits the Hund's ground multiplet 3H_4 ($J = 4$) of Pr³⁺ into a Γ_1 singlet, Γ_3 doublet, and Γ_4 and Γ_5 triplets.⁵ The non-Kramers Γ_3 doublet with a special unitary group SU(2) possesses two electric quadrupoles O_u and O_v with Γ_{3g} representation and a magnetic octupole T_{xyz} with Γ_{2u} .⁶⁻⁸ The subscript g (u) on Γ refers to even (odd) parity under time reversal. It should be noted that the Γ_3 doublet is free from magnetic dipoles J_x , J_y , and J_z with Γ_{4u} . Therefore, the nonmagnetic Γ_3 ground state is almost independent of magnetic susceptibility at low temperatures. On the other hand, an elastic constant $(C_{11}-C_{12})/2$ in Pr-based compounds with the Γ_3 ground state is generally expected to show low-temperature softening, because the $(C_{11}-C_{12})/2$ is responsible for a quadrupole susceptibility of O_v with Γ_{3g} based on CEF levels.

The degenerate Γ_3 ground state system is expected to undergo a long-range ordered state associated with a quadrupole at low temperatures, which is clearly distinguished from the magnetic ordered state. Actually, quadrupole orderings are realized in PrPtBi and PrPb₃ with the site symmetry T_d and O_h , respectively. PrPtBi shows a ferro-type quadrupole ordering at $T_Q = 1.35$ K associated with a structural phase transition to tetragonal symmetry.^{9,10} PrPb₃ exhibits an antiferro-quadrupole ordering with sinusoidal modulation at $T_Q = 0.4$ K.^{1,11-14} In these compounds, the elastic constant

$(C_{11}-C_{12})/2$ commonly displays considerable softening with decreasing temperature caused by the Γ_3 ground state and turns to increase below the quadrupole transition points because of lifting the degeneracy of the Γ_3 doublet.^{9,14} In addition, it was pointed out that a minimum around 7 K in $(C_{11}-C_{12})/2$ of PrPb₃ is attributed to an electric hexadecapole H_v with Γ_{3g} of Γ_3 doublet (0 K)– Γ_4 triplet (14.7 K)– Γ_5 triplet (28.3 K)– Γ_1 singlet (35.3 K).¹⁴

Among Pr-based compounds with the Γ_3 ground state, PrAg₂In and PrMg₃ with the site symmetry O_h are known to exhibit no sign of long-range ordering at low temperatures. PrAg₂In shows a broad peak at 0.4 K with a huge specific heat coefficient $C/T = 6.5$ J/(mol K²) without any anomaly indicating a long-range ordering down to 50 mK.¹⁵ The elastic constant $(C_{11}-C_{12})/2$ of PrAg₂In shows softening below 10 K owing to the Γ_3 ground state possessing the quadrupole O_v . Furthermore, the $(C_{11}-C_{12})/2$ reveals a minimum around 35 K. This minimum is not described by the quadrupole susceptibility of O_v based on the CEF level scheme with Γ_3 doublet (0 K)– Γ_4 triplet (71 K)– Γ_5 triplet (96 K)– Γ_1 singlet (176 K). On further lowering the temperature, the $(C_{11}-C_{12})/2$ begins to slightly increase with a $-\log T$ dependence below 90 mK.⁶

PrMg₃ is also known as the Γ_3 ground state system with a level scheme Γ_3 doublet (0 K)– Γ_4 triplet (56 K)– Γ_1 singlet (135 K)– Γ_5 triplet (183 K).^{16,17} PrMg₃ possesses a Heusler structure similar to PrAg₂In where both Ag and In sites are substituted by Mg. The specific heat of PrMg₃ exhibits a pronounced broad peak around 0.9 K with a huge specific heat coefficient $C/T = 2.8$ J/(mol K²) and indicates no sign of long-range ordering.¹⁸ The magnetic susceptibility of PrMg₃

reveals a deviation from a van Vleck term due to off-diagonal magnetic transitions from the Γ_3 ground state to the Γ_4 excited state.^{18,19} However, the characteristic feature of the elastic constant due to the Γ_3 ground state of PrMg₃ has not been investigated yet.

In the present paper, we report the elastic properties of PrMg₃ by emphasizing the characteristic behavior of $(C_{11}-C_{12})/2$. In Sec. II, sample preparation of PrMg₃ and ultrasonic measurements at low temperatures are described. The characteristic minimum and the low-temperature softening of $(C_{11}-C_{12})/2$ in PrMg₃ are presented and analyzed in terms of multipole susceptibility including electric hexadecapole as well as electric quadrupole in Sec. III. The common features of the minimum in $(C_{11}-C_{12})/2$ of PrMg₃, PrPb₃, and PrAg₂In with Γ_3 - Γ_4 states are discussed in Sec. III. A summary is presented in Sec. IV.

II. EXPERIMENTS

Single crystals of PrMg₃ were grown using the Bridgman method with a sealed Mo crucible. An x-ray photograph using a Laue camera was used to determine the orientation of the crystal axes. We prepared two single-crystal specimens of PrMg₃ No. 2 and No. 3 in the present experiment. The surfaces of the samples for the ultrasonic measurements were carefully polished to be plane parallel.

The temperature dependence of ultrasonic velocity was measured by a homemade apparatus based on a phase comparator of double-balanced mixers. Ultrasonic waves were generated and detected by piezoelectric plates of LiNbO₃ bonded on plane-parallel surfaces of the specimen. We used 36° Y-cut plates for longitudinal ultrasonic waves and X-cut plates for transverse waves. The absolute velocity v was obtained by measuring a delay time for a sequence of ultrasonic echoes with an accuracy of a few percent. Elastic constants of $C = \rho v^2$ were estimated by mass density $\rho = 3.485$ g/cm³ for PrMg₃ with a lattice constant $a = 0.7415$ nm.

A ³He-⁴He dilution refrigerator (Kelvinox, TLM) was employed for low-temperature ultrasonic measurements below 800 mK down to 20 mK, and a homemade ³He refrigerator was used for relatively higher temperature measurements above 450 mK. The temperature of the samples was measured by Cernox thin-film resistance cryogenic temperature sensors for the 140 K to 450 mK region and RuO₂ resistances for 800 mK to 20 mK.

III. RESULTS AND DISCUSSION

A. Elastic constants of PrMg₃

The temperature dependence of the elastic constants C_{11} , C_B , C_{44} , and $(C_{11}-C_{12})/2$ in PrMg₃ (No. 2) is shown in Fig. 1. The C_{11} was measured by longitudinal sound waves with frequencies of 16 MHz with a propagation vector $\mathbf{k} \parallel [001]$ and a polarization vector $\mathbf{u} \parallel [001]$. The C_{11} shows a softening below 70 K with decreasing temperature and reveals a broad minimum around 28 K. The softening in C_{11} is again observed below 10 K down to 450 mK. The $(C_{11}-C_{12})/2$ measured by transverse sound waves with frequencies

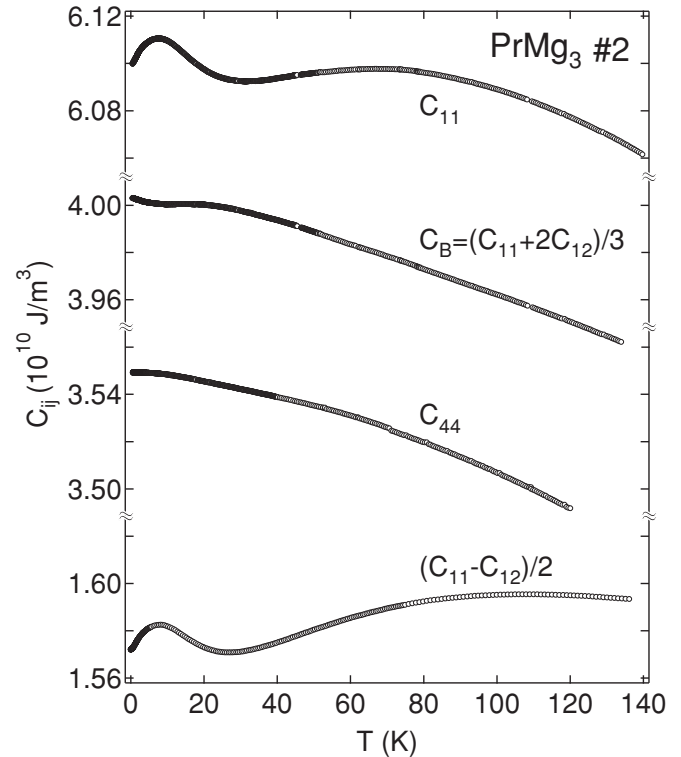


FIG. 1. Temperature dependence of the elastic constants C_{11} , C_B , C_{44} , and $(C_{11}-C_{12})/2$ in PrMg₃ (No. 2).

of 120 MHz with $\mathbf{k} \parallel [110]$ and $\mathbf{u} \parallel [1\bar{1}0]$ also exhibits a softening below 100 K with the characteristic minimum around 28 K similar to C_{11} and again shows a softening below 8 K. The softening in $(C_{11}-C_{12})/2$ causes that of C_{11} .

The transverse elastic constant C_{44} obtained using transverse sound waves with frequencies of 120 MHz with $\mathbf{k} \parallel [001]$ and $\mathbf{u} \parallel [100]$ shows a monotonic increase with decreasing temperature without anomalies. This result is accounted for by the fact that the Γ_3 doublet has no diagonal elements for the O_{xy} -type quadrupole with Γ_{5g} as $\langle \Gamma_3 | O_{xy} | \Gamma_3 \rangle = 0$.

The bulk modulus C_B is calculated from the experimental results by using a relation $C_B = C_{11} - 2(C_{11}-C_{12})/3$. The C_B reveals a monotonic increase with decreasing temperature, which indicates no anomaly in the volume change of PrMg₃.

In Fig. 2, we present the temperature dependence of $(C_{11}-C_{12})/2$ in PrMg₃ (No. 3), which is consistent with the result in PrMg₃ (No. 2) of Fig. 1. As shown in the inset of Fig. 2, $(C_{11}-C_{12})/2$ at low temperatures exhibits a shoulder-like anomaly around 200 mK and shows no sign of long-range ordering down to 20 mK. The solid line for $(C_{11}-C_{12})/2$ in Fig. 2 is a fit in terms of the multipole susceptibility including both quadrupole and hexadecapole with Γ_{3g} representation to reproduce the minimum around 28 K corresponding to half of the first Γ_4 excited energy $\Delta = 56$ K. Details are shown in the following section.

B. Analysis by multipole susceptibility

We analyze the temperature dependence of the elastic constant $(C_{11}-C_{12})/2$ for PrMg₃ in Fig. 2 in terms of the

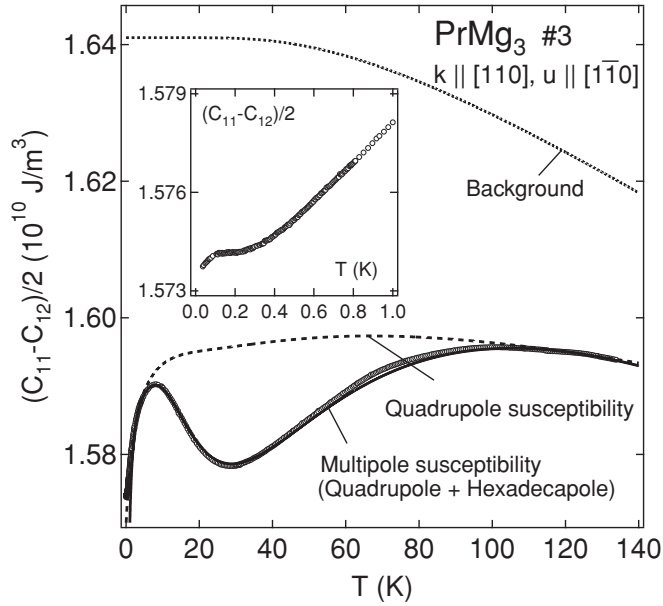


FIG. 2. Elastic constant $(C_{11}-C_{12})/2$ as a function of temperature in PrMg_3 (No. 3). The broken line is a theoretical fit by the quadrupole susceptibility with $\lambda = 0$. The solid line is a fit in terms of the multipole susceptibility of both quadrupole and hexadecapole with $\lambda = 0.0135$. The inset shows an enlarged view below 1 K.

multipole susceptibility. The CEF Hamiltonian for the ground $J = 4$ multiplet of the f^2 configuration of a Pr^{3+} ion in the cubic point symmetry is written as⁵

$$\mathcal{H}_{\text{CEF}} = \sum_{l,m} B_l^m O_l^m = B_4(O_4^0 + 5O_4^4) + B_6(O_6^0 - 21O_6^4). \quad (1)$$

Here, O_l^m is the Steven's equivalent operator.²⁰ The CEF parameters of $B_4 = -3.96 \times 10^{-2}$ K and $B_6 = -1.06 \times 10^{-3}$ K are adopted in accordance with the level scheme of Γ_3 (0 K)– Γ_4 (56 K)– Γ_1 (135 K)– Γ_5 (183 K) determined by the inelastic neutron scattering on polycrystalline PrMg_3 .¹⁷ Recently, neutron spectroscopy of a single crystal of PrMg_3 has been performed.²¹ The resultant CEF level scheme is consistent with the previous reports. The direct product of the Γ_3 doublet is reduced as a direct sum $\Gamma_3 \otimes \Gamma_3 = \Gamma_{1g} \oplus \Gamma_{2u} \oplus \Gamma_{3g}$. This implies that the Γ_3 ground state of PrMg_3 has two electric quadrupoles $O_u = (2J_z^2 - J_x^2 - J_y^2)/\sqrt{3}$ and $O_v = J_x^2 - J_y^2$ with Γ_{3g} representation and the magnetic octupole $T_{xyz} = \sqrt{15} J_x J_y J_z / 6$ with Γ_{2u} . Here, the bar means the sum of cyclic permutations on x , y , and z . Among them, the electric quadrupole O_v couples to the elastic strain $\varepsilon_v = \varepsilon_{xx} - \varepsilon_{yy}$ associated with the transverse $(C_{11}-C_{12})/2$ with $\mathbf{k} \parallel [110]$ and $\mathbf{u} \parallel [1\bar{1}0]$ in the experiment. It is expected that the present PrMg_3 system with the Γ_3 doublet– Γ_4 triplet states possesses $5^2 = 25$ multipoles, because the direct product of the quasi-quintet is reduced as $(\Gamma_3 \oplus \Gamma_4) \otimes (\Gamma_3 \oplus \Gamma_4) = 2\Gamma_{1g} \oplus \Gamma_{2u} \oplus 2\Gamma_{3g} \oplus 2\Gamma_{4u} \oplus \Gamma_{4g} \oplus 2\Gamma_{5g} \oplus \Gamma_{5u}$. It should be noted that the hexadecapoles H_u and H_v and the quadruples O_u and O_v with Γ_{3g} are relevant to the present Γ_3 – Γ_4 system. Therefore, the coupling Hamiltonian of the elastic strain ε_v of the transverse $(C_{11}-C_{12})/2$ mode to an electric

multipole \tilde{O}_v with Γ_{3g} , which is expressed by a linear combination of the quadrupole O_v and the hexadecapole H_v , is written as

$$\mathcal{H}_{MS} = -g_{\Gamma_3} \tilde{O}_v \varepsilon_v = -g_{\Gamma_3} (O_v + \lambda H_v) \varepsilon_v. \quad (2)$$

Here, g_{Γ_3} is a coupling constant and λ is the contribution ratio of the hexadecapole to the quadrupole. The hexadecapole H_v is written as²²

$$H_v = \frac{1}{4} \{ [7J_z^2 - J(J+1) - 5](J_+^2 + J_-^2) + (J_+^2 + J_-^2)[7J_z^2 - J(J+1) - 5] \}. \quad (3)$$

Here, $J_{\pm} = J_x \pm iJ_y$ are ladder operators. In Fig. 3, we show schematic views of the anisotropic charge distribution of the quadrupole O_v and the hexadecapole H_v .

The important role of the hexadecapole for the elastic properties of cubic PrSb with the Γ_1 singlet– Γ_4 triplet states (Ref. 23) and that of hexagonal PrNi_5 (Ref. 24) was previously discussed. Furthermore, the significance of the hexadecapole in the filled skutterudite $\text{PrOs}_4\text{Sb}_{12}$ with singlet-triplet states was also studied theoretically.²⁵ The hexadecapole may commonly play a significant role for the elastic properties, particularly in the Pr-based compounds with multiple degenerate states.

The softening of the present PrMg_3 is affected by the intersite interaction due to the electric multipole $\tilde{O}_v = O_v + \lambda H_v$. This multipole intersite interaction in unit volume is explained as

$$\mathcal{H}_{MM} = - \sum_{i>j} G_{\Gamma_3}^{ij} \tilde{O}_v(i) \tilde{O}_v(j) = -g'_{\Gamma_3} \sum_i (\tilde{O}_v)_i \tilde{O}_v(i). \quad (4)$$

Here, g'_{Γ_3} is the coupling constant of intersite multipole interactions in the mean-field approximation as $g'_{\Gamma_3} = zG_{\Gamma_3}^{ij}$ for an effective neighbor-site number z . The temperature dependence of the elastic constant $C_{\Gamma_3} = (C_{11}-C_{12})/2$ can be written as²⁶

$$C_{\Gamma_3}(T) = C_{\Gamma_3}^0 - \frac{N g_{\Gamma_3}^2 \chi_{\Gamma_3}(T)}{1 - g'_{\Gamma_3} \chi_{\Gamma_3}(T)}. \quad (5)$$

Here, $C_{\Gamma_3}^0$ denotes a background of the elastic constant and N is the number of Pr ions per unit volume. The multipole susceptibility of $\chi_{\Gamma_3}(T)$ is written as

$$-g_{\Gamma_3}^2 \chi_{\Gamma_3}(T) = \left\langle \frac{\partial^2 E_i}{\partial \varepsilon_v^2} \right\rangle - \frac{1}{k_B T} \left\{ \left\langle \left(\frac{\partial E_i}{\partial \varepsilon_v} \right)^2 \right\rangle - \left\langle \frac{\partial E_i}{\partial \varepsilon_v} \right\rangle^2 \right\}. \quad (6)$$

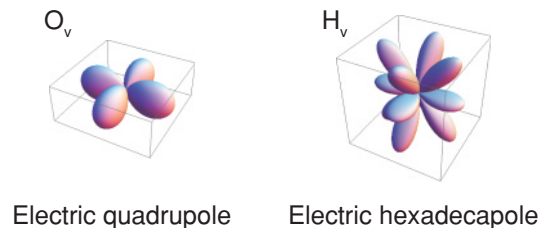


FIG. 3. (Color online) Charge distribution of the quadrupole O_v and the hexadecapole H_v with Γ_{3g} representation.

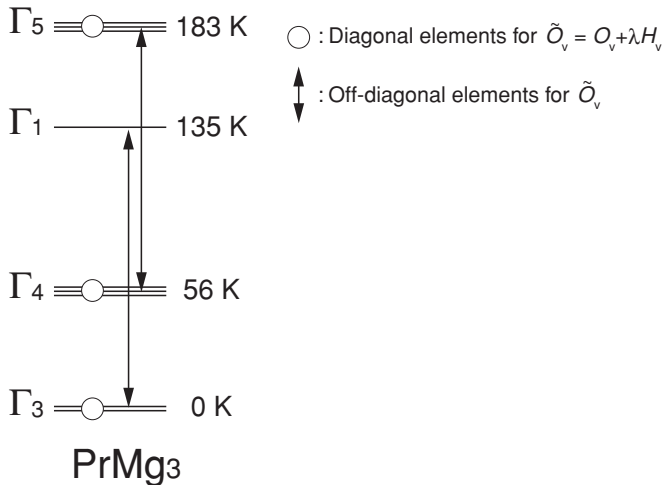


FIG. 4. CEF level scheme for the Pr^{3+} ion of PrMg_3 in point-group symmetry O_h . Circles and arrows represent selection rules for the transitions for the electric multipole moment \tilde{O}_v including the quadrupole O_v and the hexadecapole H_v with Γ_{3g} representation of Eq. (2) in the text.

Here, $\langle A \rangle$ denotes a thermal average for a physical quantity A for the CEF levels. E_i is second-order perturbation energy with respect to the elastic strain $\varepsilon_{\Gamma_3} = \varepsilon_v$ for the CEF state of PrMg_3 . The first part on the right-hand side is the van Vleck term corresponding to off-diagonal transitions, while the second part is a Curie term due to diagonal elements. The Curie term leads to sizable softening proportional to the reciprocal temperature and the van Vleck term behaves in an almost temperature independent manner at low temperatures. In the present PrMg_3 , the Curie terms of the Γ_3 ground state and the Γ_4 excited state dominate the multipole susceptibility χ_{Γ_3} in the vicinity of the characteristic minimum around 28 K of the $(C_{11}-C_{12})/2$ as shown in Fig. 4. The elastic softening in various rare-earth compounds is usually described in terms of the quadrupole susceptibility only considering the quadrupole-strain interaction. The fitting of the susceptibility in a framework of conventional quadrupole-strain interaction with $\lambda = 0$ in Eq. (2) for $(C_{11}-C_{12})/2$ of PrMg_3 is represented by a broken line in Fig. 2. This fitting succeeded well in explaining of the softening in $(C_{11}-C_{12})/2$ below 8 K, but it is rather difficult to reproduce the characteristic minimum in $(C_{11}-C_{12})/2$ around 28 K.

TABLE I. Parameters in fitting for the elastic constant $(C_{11}-C_{12})/2$ of Pr-based Γ_3 - Γ_4 systems of PrMg_3 , PrAg_2In , and PrPb_3 using multipole susceptibility with $\lambda \neq 0$ of Eq. (6).

Samples	Multipole-Strain Interaction $ g_{\Gamma_3} $	Contribution Ratio λ	Intersite Interaction g'_{Γ_3}
PrMg_3 (No. 3)	48.5 K	0.0135	-6 mK
PrAg_2In	27 K	0.0133	-4 mK
PrPb_3	45 K	0.0076	-10 mK

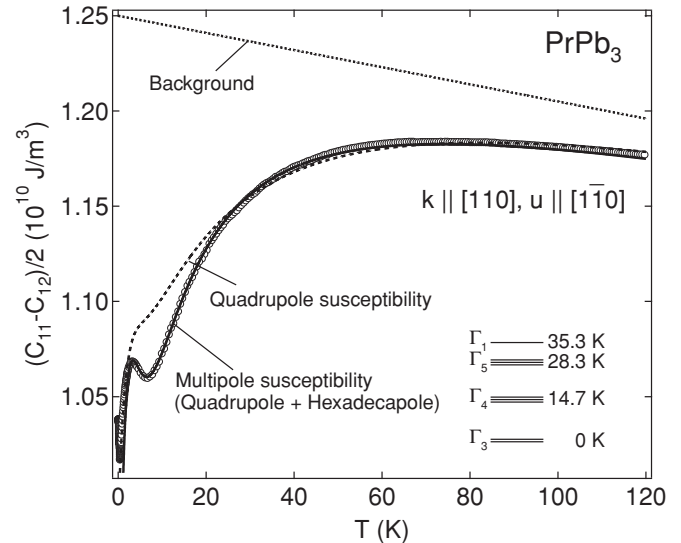


FIG. 5. Elastic constant $(C_{11}-C_{12})/2$ of PrPb_3 as a function of temperature (Ref. 28). The broken line is a fit based on the quadrupole susceptibility with $\lambda = 0$. The solid line is a fit in terms of the multipole susceptibility of both the quadrupole and hexadecapole with $\lambda = 0.0076$ in Eq. (2). The dotted line shows the background for the multipole susceptibility of Eq. (6) for $(C_{11}-C_{12})/2$.

The multipole susceptibility for the multipole-strain interaction of Eq. (2), where both the quadrupole and hexadecapole are included, successfully explains the minimum around 28 K in $(C_{11}-C_{12})/2$. The solid line in Fig. 2 is a fit with the multipole susceptibility with parameters of $|g_{\Gamma_3}| = 48.5$ K, $\lambda = 0.0135$, and $g'_{\Gamma_3} = -6$ mK for PrMg_3 (No. 3). The negative sign of g'_{Γ_3} indicates the antiferro-type multipole intersite interaction in the present PrMg_3 system. In Table I, we summarize the fitting parameters of PrMg_3 (No. 3) together with results of PrAg_2In and PrPb_3 , as will be mentioned later.

C. Comparison with other Pr-based Γ_3 - Γ_4 systems

It is worthwhile to discuss a common feature of the multipole effects across the Pr-based Γ_3 - Γ_4 systems of the present PrMg_3 , PrPb_3 , and PrAg_2In . It was reported by Nicksch *et al.*¹⁴ that PrPb_3 with the Γ_3 doublet ground state and the Γ_4 triplet excited state located at 14.7 K (Ref. 27) reveals the minimum around 7 K in the elastic constant $(C_{11}-C_{12})/2$. They already pointed out that the multipole susceptibility including both the quadrupole and hexadecapole reproduces well the characteristic minimum of $(C_{11}-C_{12})/2$. Furthermore, the other Pr-based Γ_3 - Γ_4 system of PrAg_2In also exhibits the minimum in $(C_{11}-C_{12})/2$ around 35 K.⁶ In Fig. 5, we present the fitting for PrPb_3 indicated by the solid line based on the multipole susceptibility with parameters of $|g_{\Gamma_3}| = 45$ K, $\lambda = 0.0076$, and $g'_{\Gamma_3} = -10$ mK. Here, we use ultrasonic results of PrPb_3 in our group.²⁸ The result shows essentially the same behavior as in Ref. 14. The CEF level scheme of PrPb_3 in Fig. 5 is derived from Ref. 27. The minimum around 7 K in $(C_{11}-C_{12})/2$ of PrPb_3 corresponds mostly to half of the excited energy $\Delta = 14.7$ K of the Γ_4 triplet state.

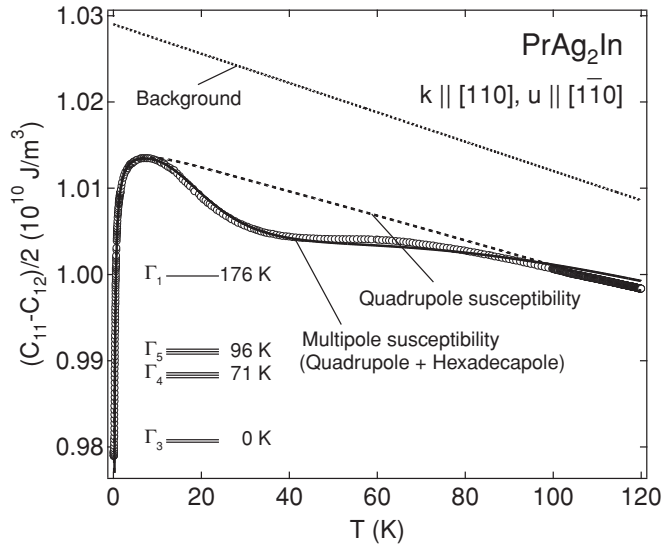


FIG. 6. Elastic constant $(C_{11}-C_{12})/2$ as a function of temperature (Ref. 6) of PrAg_2In . The broken line is a fit based on the quadrupole susceptibility with $\lambda = 0$. The solid line is a fit in terms of the multipole susceptibility of both quadrupole and hexadecapole with $\lambda = 0.0133$. The dotted line shows the background for the multipole susceptibility of Eq. (6) for $(C_{11}-C_{12})/2$.

The characteristic minimum around 35 K in $(C_{11}-C_{12})/2$ of PrAg_2In in Fig. 6 of Ref. 6 is also well reproduced by the solid line of the multipole susceptibility with $|g_{\Gamma_3}| = 27$ K, $\lambda = 0.0133$, and $g'_{\Gamma_3} = -4$ mK. The CEF levels of PrAg_2In in our Fig. 6 is derived from the results of neutron scatterings in Ref. 29. This minimum in $(C_{11}-C_{12})/2$ of PrAg_2In , as well as in the cases of PrPb_3 and the present PrMg_3 , corresponds to half of the splitting energy $\Delta = 71$ K of the Γ_4 triplet excited state.

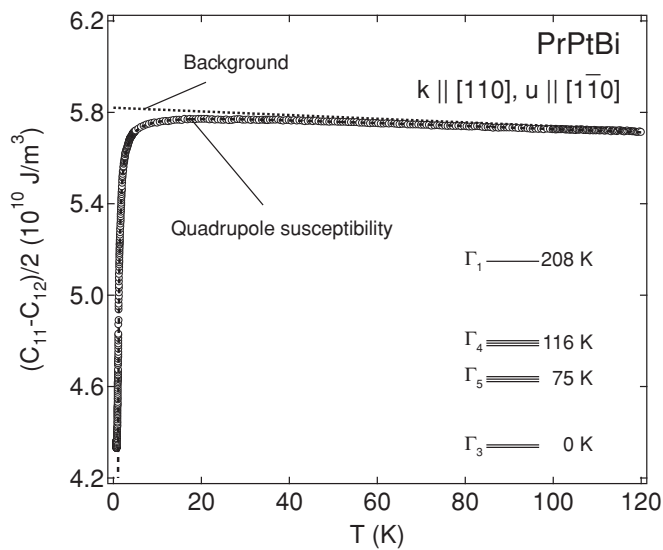


FIG. 7. Elastic constant $(C_{11}-C_{12})/2$ as a function of temperature for PrPtBi (Ref. 30). The broken and dotted lines show a fit by quadrupole susceptibility with $\lambda = 0$ and the background of $(C_{11}-C_{12})/2$, respectively.

On the other hand, it is notable that $(C_{11}-C_{12})/2$ of PrPtBi with the Γ_3 ground state and the first excited Γ_5 triplet state located at 75 K shows no apparent minimum as shown in Fig. 7 in Ref. 30. The broken line in our Fig. 7 by a fit in terms of the quadrupole susceptibility with $|g_{\Gamma_3}| = 30$ K, $\lambda = 0$, and $g'_{\Gamma_3} = 38$ mK reproduces the experimental result of PrPtBi . Here, we used the CEF levels of Fig. 7 in Ref. 10. According to the group theoretical viewpoint, the quasi-quintet of $\Gamma_3 \oplus \Gamma_5$ possesses the quadrupole and the hexadecapole with Γ_{3g} representation as well. The $(C_{11}-C_{12})/2$ of PrPtBi with Γ_3 - Γ_5 states shows no obvious minimum, which is markedly different from the minimum of $(C_{11}-C_{12})/2$ of PrMg_3 , PrPb_3 , and PrAg_2In with Γ_3 - Γ_4 states.

It is worthwhile to compare the elastic softening for the Γ_3 - Γ_4 system in Fig. 8(a) and that for the Γ_3 - Γ_5 in Fig. 8(b) by using the multipole susceptibility as

$$-\chi_{\Gamma_3}^{(3,i)} \Delta = -\frac{2\Delta}{k_B T Z} \left[\langle \Gamma_3 | \tilde{O}_v | \Gamma_3 \rangle^2 + \langle \Gamma_i | \tilde{O}_v | \Gamma_i \rangle^2 \right] \times \exp\left(-\frac{\Delta}{k_B T}\right) \quad (i = 4 \text{ or } 5), \quad (7)$$

where Z is the partition function for the corresponding levels. We consider only low-lying states of the Γ_3 doublet ground state and the Γ_4 or Γ_5 triplet excited state located at Δ K for simplicity. We adopt the same ratio $\lambda = 0.01$ for both calculations to examine the contribution of the hexadecapole to the appearance of the minimum in the temperature dependence

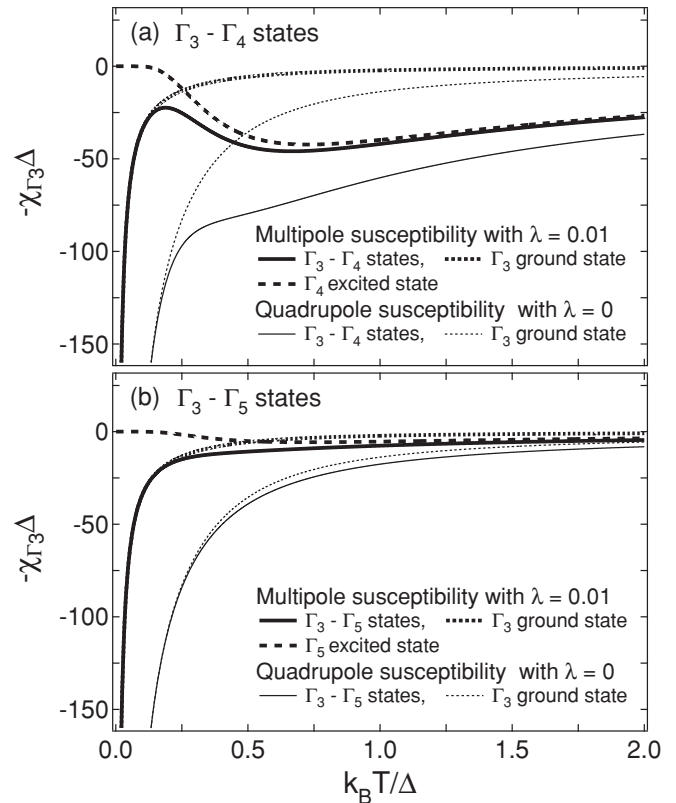


FIG. 8. Temperature dependence of the multipole susceptibilities of Eq. (7) in the text with $\lambda = 0.01$ in $(C_{11}-C_{12})/2$ for the systems with Γ_3 doublet- Γ_4 triplet states in (a) and Γ_3 doublet- Γ_5 triplet states in (b).

of $(C_{11}-C_{12})/2$. The matrix elements for both the quadrupole O_v and hexadecapole H_v of Pr^{3+} ($J = 4$) ion in the cubic symmetry are presented in the Appendix.

It should be noted that the multipole susceptibility for the Curie term of the Γ_4 excited state with $\langle \Gamma_4^\alpha | \tilde{O}_v | \Gamma_4^\alpha \rangle = 12.95$, $\langle \Gamma_4^\beta | \tilde{O}_v | \Gamma_4^\beta \rangle = 0$, and $\langle \Gamma_4^\gamma | \tilde{O}_v | \Gamma_4^\gamma \rangle = -12.95$, shown by a thick broken line in Fig. 8(a), indicates the significant minimum around $\Delta/2$ K corresponding to that of the experimental results of $(C_{11}-C_{12})/2$ in PrMg_3 , PrPb_3 , and PrAg_2In with Γ_3 - Γ_4 states. Such behavior possessing the minimum is also seen in the quadrupole susceptibility due to the Γ_4 excited state with $\langle \Gamma_4^\alpha | O_v | \Gamma_4^\alpha \rangle = 14$, $\langle \Gamma_4^\beta | O_v | \Gamma_4^\beta \rangle = 0$, and $\langle \Gamma_4^\gamma | O_v | \Gamma_4^\gamma \rangle = -14$ (not shown here). However, the quadrupole susceptibility for Γ_3 - Γ_4 states shows only a weak shoulder around $\Delta/2$ K as represented by a thin solid line in Fig. 8(a), because the elastic softening due to the Γ_3 ground state with $\langle \Gamma_3^\alpha | O_v | \Gamma_3^\alpha \rangle = 8/\sqrt{3}$ and $\langle \Gamma_3^\beta | O_v | \Gamma_3^\beta \rangle = -8/\sqrt{3}$ is dominant at low temperatures as shown by a thin dotted line in Fig. 8(a).

When we take account of the hexadecapole in addition to the quadrupole, the multipole susceptibility for Γ_3 - Γ_4 states shows a clear minimum as shown by a thick solid line in Fig. 8(a). This occurs because the susceptibility for the Curie term of the Γ_3 doublet with $\langle \Gamma_3^\alpha | \tilde{O}_v | \Gamma_3^\alpha \rangle = 3.2/\sqrt{3}$ and $\langle \Gamma_3^\beta | \tilde{O}_v | \Gamma_3^\beta \rangle = -3.2/\sqrt{3}$ as shown by a thick dotted line reveals shifting to lower temperatures compared to that for the Curie term with $\langle \Gamma_3^\alpha | O_v | \Gamma_3^\alpha \rangle$ and $\langle \Gamma_3^\beta | O_v | \Gamma_3^\beta \rangle$ as shown by the thin dotted line in Fig. 8(a).

Furthermore, the Curie term due to the Γ_5 excited triplet with $\langle \Gamma_5^\alpha | \tilde{O}_v | \Gamma_5^\alpha \rangle = 4.75$, $\langle \Gamma_5^\beta | \tilde{O}_v | \Gamma_5^\beta \rangle = 0$, and $\langle \Gamma_5^\gamma | \tilde{O}_v | \Gamma_5^\gamma \rangle = -4.75$ makes a relatively small contribution in comparison with that due to the Γ_4 excited triplet. Consequently, the minimum in the temperature dependence of $(C_{11}-C_{12})/2$ is expected to emerge in the Γ_3 - Γ_4 system, but is irrelevant for the Γ_3 - Γ_5 system.

IV. SUMMARY

In the present study, we have performed ultrasonic measurements of the Pr-based compound PrMg_3 with the Γ_3

doublet ground state and Γ_4 triplet first excited state located at 54 K. The characteristic minimum around 28 K and pronounced softening below 8 K are observed in the transverse elastic constant $(C_{11}-C_{12})/2$. The multipole susceptibility including the hexadecapole H_v as well as the quadrupole O_v with Γ_{3g} representation describes well the minimum and the following softening in $(C_{11}-C_{12})/2$. The common feature of the minimum in $(C_{11}-C_{12})/2$ for the pseudo-quintet Γ_3 - Γ_4 systems of PrMg_3 in the present experiments and PrPb_3 and PrAg_2In in previous research arises from the multipole susceptibility. In contrast, the $(C_{11}-C_{12})/2$ of PrPtBi with the Γ_3 ground state and the Γ_5 triplet first excited state shows no apparent minimum, because the matrix elements of $\tilde{O}_v = O_v + \lambda H_v$ for the Γ_5 state are smaller than those of the Γ_4 state. The higher rank hexadecapole, as well as the quadrupole, plays a significant role in the elastic properties of the Pr-based Γ_3 - Γ_4 multiply degenerated systems.

ACKNOWLEDGMENTS

This work was supported by a Grant-in-Aid for Specially Promoted Research (No. 18002008) ‘‘Strongly correlated quantum phases associated with charge fluctuations’’ from the Ministry of Education, Culture, Sports, and Technology of Japan. One of the authors (K.A.) appreciates financial support by Research Fellows of the Japan Society for the Promotion of Science for Young Scientists. The authors are grateful to B. Lüthi for his valuable discussions on the present work.

APPENDIX: MATRIX ELEMENTS FOR THE QUADRUPOLE O_v AND HEXADECAPOLE H_v

This Appendix gives matrix elements for the quadrupole O_v and the hexadecapole H_v of the Pr^{3+} ($J = 4$) ion in the cubic point symmetry. The eigenstates for $J = 4$ of Pr^{3+} ion in the cubic system are chosen to be diagonal for H_{CEF} of Eq. (1) in Ref. 5. In the present paper, however, we adopt alternative eigenstates for the diagonal matrices of the quadrupole O_v and hexadecapole H_v of Eq. (3).

$$O_v = \begin{pmatrix} \langle \Gamma_1 | \\ \langle \Gamma_3^\alpha | \\ \langle \Gamma_3^\beta | \\ \langle \Gamma_4^\alpha | \\ \langle \Gamma_4^\beta | \\ \langle \Gamma_4^\gamma | \\ \langle \Gamma_5^\alpha | \\ \langle \Gamma_5^\beta | \\ \langle \Gamma_5^\gamma | \end{pmatrix} \begin{pmatrix} |\Gamma_1\rangle & |\Gamma_3^\alpha\rangle & |\Gamma_3^\beta\rangle & |\Gamma_4^\alpha\rangle & |\Gamma_4^\beta\rangle & |\Gamma_4^\gamma\rangle & |\Gamma_5^\alpha\rangle & |\Gamma_5^\beta\rangle & |\Gamma_5^\gamma\rangle \\ 0 & 4\sqrt{\frac{35}{6}} & -4\sqrt{\frac{35}{6}} & 0 & 0 & 0 & 0 & 0 & 0 \\ 4\sqrt{\frac{35}{6}} & \frac{8}{\sqrt{3}} & 0 & 0 & 0 & 0 & 0 & 0 & 0 \\ -4\sqrt{\frac{35}{6}} & 0 & -\frac{8}{\sqrt{3}} & 0 & 0 & 0 & 0 & 0 & 0 \\ 0 & 0 & 0 & 14 & 0 & 0 & 0 & 0 & \sqrt{7} \\ 0 & 0 & 0 & 0 & 0 & 0 & 0 & 2\sqrt{7} & 0 \\ 0 & 0 & 0 & 0 & 0 & -14 & -\sqrt{7} & 0 & 0 \\ 0 & 0 & 0 & 0 & 0 & -\sqrt{7} & 4 & 0 & 0 \\ 0 & 0 & 0 & 0 & 2\sqrt{7} & 0 & 0 & 0 & 0 \\ 0 & 0 & 0 & \sqrt{7} & 0 & 0 & 0 & 0 & -4 \end{pmatrix}, \quad (\text{A1})$$

$$H_v = \begin{pmatrix} \langle \Gamma_1 | \\ \langle \Gamma_3^\alpha | \\ \langle \Gamma_3^\beta | \\ \langle \Gamma_4^\alpha | \\ \langle \Gamma_4^\beta | \\ \langle \Gamma_4^\gamma | \\ \langle \Gamma_5^\alpha | \\ \langle \Gamma_5^\beta | \\ \langle \Gamma_5^\gamma | \end{pmatrix} \begin{pmatrix} |\Gamma_1\rangle & |\Gamma_3^\alpha\rangle & |\Gamma_3^\beta\rangle & |\Gamma_4^\alpha\rangle & |\Gamma_4^\beta\rangle & |\Gamma_4^\gamma\rangle & |\Gamma_5^\alpha\rangle & |\Gamma_5^\beta\rangle & |\Gamma_5^\gamma\rangle \\ 0 & 12\sqrt{\frac{35}{6}} & -12\sqrt{\frac{35}{6}} & 0 & 0 & 0 & 0 & 0 & 0 \\ 12\sqrt{\frac{35}{6}} & -160\sqrt{3} & 0 & 0 & 0 & 0 & 0 & 0 & 0 \\ -12\sqrt{\frac{35}{6}} & 0 & 160\sqrt{3} & 0 & 0 & 0 & 0 & 0 & 0 \\ 0 & 0 & 0 & -105 & 0 & 0 & 0 & 0 & 45\sqrt{7} \\ 0 & 0 & 0 & 0 & 0 & 0 & 0 & 90\sqrt{7} & 0 \\ 0 & 0 & 0 & 0 & 0 & 105 & -45\sqrt{7} & 0 & 0 \\ 0 & 0 & 0 & 0 & 0 & -45\sqrt{7} & 75 & 0 & 0 \\ 0 & 0 & 0 & 0 & 90\sqrt{7} & 0 & 0 & 0 & 0 \\ 0 & 0 & 0 & 45\sqrt{7} & 0 & 0 & 0 & 0 & -75 \end{pmatrix}, \quad (\text{A2})$$

$$\begin{aligned} |\Gamma_1\rangle &= \sqrt{\frac{5}{24}}(|+4\rangle + |-4\rangle) + \sqrt{\frac{7}{12}}|0\rangle, \\ |\Gamma_3^\alpha\rangle &= -\sqrt{\frac{7}{48}}(|+4\rangle + |-4\rangle) + \frac{1}{2}(|+2\rangle + |-2\rangle) + \sqrt{\frac{5}{24}}|0\rangle, \\ |\Gamma_3^\beta\rangle &= -\sqrt{\frac{7}{48}}(|+4\rangle + |-4\rangle) - \frac{1}{2}(|+2\rangle + |-2\rangle) + \sqrt{\frac{5}{24}}|0\rangle, \\ |\Gamma_4^\alpha\rangle &= -\frac{1}{4}(|+3\rangle + |-3\rangle) - \frac{\sqrt{7}}{4}(|+1\rangle + |-1\rangle), \\ |\Gamma_4^\beta\rangle &= \sqrt{\frac{1}{2}}(|+4\rangle - |-4\rangle), \\ |\Gamma_4^\gamma\rangle &= \frac{1}{4}(|+3\rangle - |-3\rangle) - \frac{\sqrt{7}}{4}(|+1\rangle - |-1\rangle), \\ |\Gamma_5^\alpha\rangle &= \frac{\sqrt{7}}{4}(|+3\rangle - |-3\rangle) + \frac{1}{4}(|+1\rangle - |-1\rangle), \\ |\Gamma_5^\beta\rangle &= \sqrt{\frac{1}{2}}(|+2\rangle - |-2\rangle), \\ |\Gamma_5^\gamma\rangle &= -\frac{\sqrt{7}}{4}(|+3\rangle + |-3\rangle) + \frac{1}{4}(|+1\rangle + |-1\rangle). \end{aligned} \quad (\text{A3})$$

Here, $|J_z\rangle$ of Eq. (A3) denotes the eigenket for the z component of total angular momentum $J = 4$.

*araki@phys.sc.niigata-u.ac.jp

¹T. Onimaru, T. Sakakibara, N. Aso, H. Yoshizawa, H. S. Suzuki, and T. Takeuchi, *Phys. Rev. Lett.* **94**, 197201 (2005).

²H. Sugawara, T. D. Matsuda, K. Abe, Y. Aoki, H. Sato, S. Nojiri, Y. Inada, R. Settai, and Y. Ōnuki, *J. Magn. Magn. Mater.* **226–230**, 48 (2001).

³E. D. Bauer, N. A. Frederick, P.-C. Ho, V. S. Zapf, and M. B. Maple, *Phys. Rev. B* **65**, 100506 (2002).

⁴T. Goto, Y. Nemoto, K. Sakai, T. Yamaguchi, M. Akatsu, T. Yanagisawa, H. Hazama, K. Onuki, H. Sugawara, and H. Sato, *Phys. Rev. B* **69**, 180511 (2004).

⁵K. R. Lea, M. J. M. Leask, and W. P. Wolf, *J. Phys. Chem. Solids.* **23**, 1381 (1962).

⁶O. Suzuki, H. S. Suzuki, H. Kitazawa, G. Kido, T. Ueno, T. Yamaguchi, Y. Nemoto, and T. Goto, *J. Phys. Soc. Jpn.* **75**, 013704 (2006).

⁷R. Shiina, H. Shiba, and P. Thalmeier, *J. Phys. Soc. Jpn.* **66**, 1741 (1997).

⁸Y. Kuramoto, H. Kusunose, and A. Kiss, *J. Phys. Soc. Jpn.* **78**, 072001 (2009).

⁹H. Suzuki, M. Kasaya, T. Miyazaki, Y. Nemoto, and T. Goto, *J. Phys. Soc. Jpn.* **66**, 2566 (1997).

¹⁰M. Kasaya, H. Suzuki, D. Tazawa, M. Shirakawa, A. Sawada, and T. Osakabe, *Physica B* **281–282**, 579 (2000).

¹¹W. Gross, K. Knorr, A. P. Murani, and K. H. Buschow, *Z. Phys. B* **37**, 123 (1980).

¹²E. Bucher, K. Andres, A. C. Gossard, and J. P. Maita, *J. Low Temp.* **2**, 322 (1972).

¹³P. Morin, D. Schmitt, and E. du Tremolet de Lacheisserie, *J. Magn. Magn. Mater.* **30**, 257 (1982).

¹⁴M. Nicksch, W. Assmus, B. Lüthi, H. R. Ott, and J. K. Kjems, *Helv. Phys. Acta* **55**, 688 (1982).

- ¹⁵A. Yatskar, W. P. Beyermann, R. Movshovich, and P. C. Canfield, *Phys. Rev. Lett.* **77**, 3637 (1996).
- ¹⁶A. Andreeff, E. A. Goremychkin, H. Griessmann, B. Lippold, W. Matz, O. D. Chistyakov, and E. M. Savitskii, *Phys. Status Solidi B* **98**, 283 (1980).
- ¹⁷R. M. Galera, A. P. Murani, and J. Pierre, *J. Magn. Magn. Mater.* **23**, 317 (1981).
- ¹⁸H. Tanida, H. S. Suzuki, S. Takagi, H. Onodera, and K. Tanigaki, *J. Phys. Soc. Jpn.* **75**, 073705 (2006).
- ¹⁹T. Morie, T. Sakakibara, H. S. Suzuki, H. Tanida, and S. Takagi, *J. Phys. Soc. Jpn.* **78**, 033705 (2009).
- ²⁰K. W. H. Stevens, *Proc. Phys. Soc. London A* **65**, 209 (1952).
- ²¹H. S. Suzuki, R. M. Galera, M. Amara, L. P. Regnault, T. J. Sato, H. Tanida, and S. Takagi, *J. Phys.: Conf. Ser.* **150**, 042196 (2009).
- ²²E. R. Callen, and H. B. Callen, *Phys. Rev.* **129**, 578 (1963).
- ²³B. Lüthi, M. Nicksch, R. Takke, W. Assmus, and W. Grill, in *Crystalline Electric Field Effects in f-Electron Magnetism*, edited by R. P. Guertin, W. Suski, and Z. Zolnierrek (Plenum, New York, 1982).
- ²⁴T. Udagawa, S. Hashio, K. Morita, O. Suzuki, A. Tamaki, T. Takamasu, S. Kato, H. Kitazawa, and G. Kido, *J. Phys. Soc. Jpn.* **73**, 1514 (2004).
- ²⁵R. Shiina, *J. Phys. Soc. Jpn.* **73**, 2257 (2004).
- ²⁶B. Lüthi, *Physical Acoustics in the Solid State* (Springer, 2005).
- ²⁷T. Tayama, T. Sakakibara, K. Kitami, M. Yokoyama, K. Tenya, H. Amitsuka, D. Aoki, Y. Ōnuki, and Z. Kletowski, *J. Phys. Soc. Jpn.* **70**, 248 (2001).
- ²⁸S. Jumonji, master's thesis, Graduate School of Science and Technology, Niigata University, 2006 (in Japanese).
- ²⁹T. M. Kelley, W. P. Beyermann, R. A. Robinson, F. Trouw, P. C. Canfield, and H. Nakotte, *Phys. Rev. B* **61**, 1831 (2000).
- ³⁰K. Sakai, master's thesis, Graduate School of Science and Technology, Niigata University, 2003 (in Japanese).